Monte Carlo simulations of radiative heat exchange in a street canyon with trees

Zhi-Hua Wang*

School of Sustainable Engineering and the Built Environment, Arizona State University

Tempe, AZ 85287, *USA*

* Email: zhwang@asu.edu. Tel: +1-480-727-2933; Fax: +1-480-965-0557

Abstract

Land surface energy balance in a built environment is widely modelled using urban canopy models with representation of building arrays as a big street canyon. Modification of this simplified geometric representation, on the other hand, leads to challenging numerical difficulties in improving physical parameterization schemes that are deterministic in nature. In this paper, we develop a stochastic algorithm to estimate view factors between canyon facets in the presence of shade trees based on Monte Carlo simulation, where an analytical formulation is inhibited by the complex geometry. The model is validated against analytical solutions of benchmark radiative problems as well as field measurements in real street canyons. In conjunction with the matrix method resolving infinite number of reflections, the proposed model is capable of predicting the radiative exchange inside the street canyon with good accuracy. Modeling of transient evolution of thermal filed inside the street canyon using the proposed method demonstrate the potential of shade trees in mitigating canyon surface temperatures as well as saving of building energy use. This new numerical framework also deepens our insight into the fundamental physics of radiative heat transfer and surface energy balance for urban climate modeling.

Keywords: *Building energy consumption; Monte Carlo method; Radiative heat transfer; View factors*

1. Introduction

Today, urban areas are home to more than half of the world's population, with a projected urban population of 6.3 billion (68% total global population) in 2050 (United Nations, 2012). Complex landscape characteristics presented in a built environment has led to significant modification of surface partitioning of solar energy. Urban areas therefore have higher environmental temperatures than their rural surroundings, a well-known phenomenon as the "urban heat island" (UHI) (Oke, 1982; Taha, 1997; Arnfield, 2003). As a consequence, urban climate, as largely dictated by functions of manmade infrastructure and human stressors, has paramount effect on energy consumption in cities (Santamouris et al., 2001; Kikegawa et al., 2003). The past decade has seen increasing effort in reducing the impact of UHI on energy use with various mitigation strategies such as the use of cool pavements, green roofs, and shade trees (Akbari et al., 2001; Ouldboukhitine et al., 2014; Santamouris, 2014). Understanding the fundamental physics governing the working mechanisms of these strategies, especially on how they change the surface energy balance in urban canopies, is becoming increasingly pressing to researchers.

In addition to thermal and optical properties of pavement materials (Sailor et al., 2006; Synnefa et al., 2007), urban morphology plays a critical role in dictating UHI intensity and has a significant impact on building energy consumption (Wong et al., 2011). In particular, the geometry and density of building arrays are important contributors to the surface energy balance of built environments through radiative trapping and shading effects (Harman et al., 2004; Wang et al., 2011b). Radiosity algorithms have been developed to predict surface irradiance and interior illumination in urban environments (Robinson and Stone, 2005; 2006). Contributions of radiance from discretized patches,

partially obscured by the canyon geometry and presence of obstructions, are predicted using ray-tracing methods, and the associated view factors can be estimated. Radiosity methods exhibit good accuracy in predicting radiative transfer at building-revolving scales (with spatial resolutions < 10 km), as compared to other radiation models (Robinson and Stone, 2004).

This study, on the other hand, focuses on the development of a radiative transfer model in urban canopies that will later be incorporated into numerical weather predictions of urban areas at city scales (with spatial resolutions ~10 – 100 km). At these large scales, numerical urban land surface models do not resolve detailed building and street canyon geometries, but rather resort to simplified representations. Currently, two broad types of representations of a "generic" urban area are adopted, viz. as a two dimensional (2D) street canyon (Nunez and Oke, 1976), or a three dimensional (3D) rectangular block (Aoyagi and Takahash, 2012). With these simplified geometric representations, building arrays are usually resolved by normalized roof, wall and road dimensions for 2D canyons (Kusaka et al., 2001), or by roof and frontal areas for 3D blocks (Grimmond and Oke, 1999). Currently, most urban surface energy models are based on the 2D street canyon representation of urban areas, e.g. the urban canopy models (UCM) adopted in the widely-used Weather Research and Forecasting (WRF) platform (Chen et al., 2011). With this geometric simplification, radiative heat exchange in urban areas can be analytically resolved based on the view factors among urban facets (sky, ground, and walls). While the 2D street canyon representation of a built terrain is attractive due to its geometric simplicity, any incremental modification to the geometry can lead to laborious effort or even formidable challenges in modifying physical parameterizations of UCMs.

Of particular importance to this study, recent advances in urban climate modeling demonstrate that it is critical to include urban vegetation and the associated hydrological processes for UCMs to realistically capture the surface energy budgets, especially the latent heat (Grimmond et al., 2010, 2011). This requirement has led to new urban parameterization schemes that integrate urban vegetation, grass or trees, in street canyons to enable direct soil-vegetation-atmosphere interactions (Lemonsu et al., 2012; Wang et al., 2013). On the other hand, these changes necessarily bring up new modeling challenges, such as how the shading effect of trees in a street canyon can be realistically represented? Analytical formulation of view factors with the presence of trees in a street canyon will be extremely difficult, if not impossible, given a variety of geometry of trees, needless to mention their spatial locations and sizes. In addition, degraded air quality in urban areas can modify the optical and radiative properties in the canopy layer (Prabhakar et al., 2014) and challenge the assumption of air as a non-participating (transparent, non-scattering, and non-absorbing) medium for radiative transfer in urban areas. This is particularly concerned for cities with severe pollution, e.g. heavy PM 2.5, PM 10 and aerosol loads in megacities in northern China (Sun et al., 2006; Li et al., 2007).

To address these new challenges, one naturally resorts to stochastic approaches based on random sampling, e.g. a Monte Carlo method. Monte Carlo simulations of radiative heat transfer have a long history of development (Howell, 1968, 1998; Yang et al. 1995). While its advantage may not be obvious for problems with simple geometries and ideal transmitting media, Monte Carlo is an excellent technique for modeling complex terrains and anthropogenic sources of emissions presented in highly urbanized environments. The main advantage of Monte Carlo is that when the problem complexity increases, the

numerical expense of analytical methods involving mathematical integration of radiative transport equation increases exponentially, while that of Monte Carlo procedures only increases linearly (Howell, 1968). In the literature, only a handful number of Monte Carlo methods were available for radiative heat transfer in street canyons. The most recent model by Krayenhoff et al. (2014) is probably the only one that takes into account the presence of trees in urban canopies. However, their work was developed for a multi-layer UCM with probabilistic distribution of building heights, and there was a lack of comparison to field measurements.

In this paper, we derive a Monte Carlo algorithm for radiative exchange in 2D street canyons, incorporating the presence of trees (or generic obstacles alike) and their shading effect. In combination with matrix method for infinite radiative reflections as well as analytical method for heat conduction through the building envelope, a new modeling framework is developed for capturing energy balance inside a street canyon with realistic representation of radiative exchange based on stochastic procedures. The proposed method is validated against benchmark radiative transfer problems using analytical method, as well as in-situ measurements in urban areas. The validated model is then applied to study the effect of various canyon and tree geometries on the radiative exchange in a street canyon. Shading effect of trees lead to reduced surface temperature of canyon facets (walls and roads), as well as potential saving of building energy.

The proposed method for radiative exchange is developed for a simplified 2D “big canyon” with particular applications to numerical weather prediction of urban areas at large (neighborhood to city) scales, via incorporation into the widely used WRF-UCM platform. With improved model accuracy of resolving radiative heat fluxes as well as

surface temperatures at each canyon facet, the proposed method will enhance the predictability of the overall numerical framework on other surface energy budgets, viz. sensible and latent heat and thermal storage in built environments. Future development and applications of this numerical framework will also help to provide useful guidelines for urban landscape management and sustainable urban planning in terms of, e.g. solar energy harvest, heat island mitigation, and/or building energy efficiency.

2. Model algorithms

In this section, we present the detailed algorithms and formulation of the proposed numerical framework, including the Monte Carlo method for estimating view factors in a street canyon with shade trees, and the matrix inversion for resolution of infinite reflections among canyon facets. Note that the proposed method is developed for longwave (diffuse) thermal radiation, which is appropriate for street canyons with direct solar irradiance shaded by obstructions and trees.

2.1. Monte Carlo method for radiative view factors

Consider an energy bundle (radiative "ray") between two generic surfaces, as shown in Fig. 1, emitting from surface 1 and received by surface 2. The radiative view factors F_{12}, with a ray radiated from a generic area A_1 and incident on another generic area A_2, is given by,

$$F_{12} = \frac{1}{A_1}\int_{A_1}\int_{A_2} \frac{\cos\eta_1 \cos\eta_2}{\pi S^2} dA_2 dA_1 , \qquad (1)$$

where η_1 and η_2 are the angle between the ray and the surface normal of A_1 and A_2, respectively; and S is the path length of the ray. Properties that must be satisfied by view factors matrix include: self-view factor for a flat facet must be zero, and no radiant energy can be lost, i.e.

$$F_{ii} = 0, \text{ no summation over } i; \ \sum_{j=1}^{N} F_{ij} = 1. \tag{2}$$

In addition, the reciprocal relation holds, i.e.

$$A_1 F_{12} = A_2 F_{21}. \tag{3}$$

In particular, the view factors between the four urban facets of the 2D street canyon (the "sky", two walls, and the road, without trees) can be solved by analytical integration, and are given by (Sparrow and Cess, 1978)

$$F_{SG} = F_{GS} = \sqrt{1+\left(\frac{H}{W}\right)^2} - \frac{H}{W}, \tag{4}$$

$$F_{WW} = \sqrt{1+\left(\frac{W}{H}\right)^2} - \frac{W}{H}, \tag{5}$$

$$F_{SW} = F_{GW} = \frac{1}{2}\left[1 - \sqrt{1+\left(\frac{H}{W}\right)^2} + \frac{H}{W}\right], \tag{6}$$

$$F_{WS} = F_{WG} = \frac{1}{2}\left[1 - \sqrt{1+\left(\frac{W}{H}\right)^2} + \frac{W}{H}\right], \tag{7}$$

where subscripts *S*, *G*, and *W* denote sky, ground, and wall, respectively, *H* is the building height, and *W* is the width of canyon, as shown in Figure 2.

It is straightforward to verify that the analytical formulas observe the properties of view factors in Eqs. (2)-(3). Analytical formulas of view factors, such as Eqs. (4)-(7), are

handy to use but may become difficult to formulate in more complex problems. For example, analytical computation of view factors for a street canyon with trees, as shown in Figure 2, is hitherto absent (Krayenhoff et al., 2014). The Monte Carlo method, on the other hand, invokes a probabilistic sampling of all rays emitted from surface by taking a "random walk", and avoids the difficulty inherent in the integration process of Eq. (1) for complex geometry (Howell, 1968). To randomize the radiative exchange process, the direction of the emitted bundle can be determined by the polar angle θ_1 and the azimuthal angle η_1, each associated with a random number R_θ and R_η as:

$$R_\theta = \frac{\theta_1}{2\pi}, \tag{8}$$

$$\sqrt{R_\eta} = \sin\eta_1 . \tag{9}$$

The emitting coordinates of all four canyon facets of a 2D street canyon, are given by

$$x_e = WR_x; \qquad z_e = HR_z, \tag{10}$$

where R_x and R_z are the random numbers associated with emitting coordinates x_e and z_e from a given canyon facet in x and z directions, respectively, W the canyon width, and H the wall height. To track the incident location of a ray transfer between two parallel surfaces, only one coordinate will be involved. From the geometry, it is straightforward to show that between ground and sky, and the two parallel walls

$$x_i = x_e + H\tan\eta_1\cos\theta_1, \text{ between sky and ground}, \tag{11}$$

$$z_i = z_e + W\tan\eta_1\cos\theta_1, \text{ between walls}, \tag{12}$$

The incident coordinates of a ray transferring between two perpendicular surfaces are slightly more complicated, as given by

$$x_i = \frac{z_e}{\tan\eta_1 \cos\theta_1}, \text{ from walls to sky/ground}, \tag{13}$$

$$z_i = \frac{x_e}{\tan\eta_1 \cos\theta_1}, \text{ from sky/ground to walls}, \tag{14}$$

Tracing a ray emitting from surface A_1 with random motion, it is relatively straightforward to see if it actually absorbed by surface A_2 using Monte Carlo algorithm, by checking the incident coordinates. For example, if the incidental horizontal coordinate falls within the spatial location of ground, i.e. $0 \le x_i \le W$, the emitted ray is considered as received by the ground; it is "missed" by the ground otherwise.

2.2. Matrix solution of net radiation

Given *i*-th facet in a street canyon, with $1 \le i \le N$ and N the total number of facets, it is associated with a range of radiative fluxes, namely the irradiance (i.e. the total incoming radiation) I_i, the radiosity (the total outgoing) J_i, the emittance (the total emitted) M_i, and the net radiative flux Q_i, respectively. Assuming all facets are opaque, these fluxes are not independent but related by

$$I_i = \sum_{j=1}^{N} J_j F_{ji}, \tag{15}$$

$$J_i = M_i + (1-\varepsilon_i) I_i, \tag{16}$$

$$Q_i = M_i - J_i, \tag{17}$$

where subscripts '*i*' and '*j*' are facet indices, ε is the emissivity and F_{ji} are the view factors for radiation transfer from *j*-th to *i*-th surface, as defined in Eq. (1).

The quantity of interest is the net radiation flux, which involves the radiosity from *other* facets incident on the surface of interest. Combining Eqs. (15) and (16), we have

$$J_i = M_i + (1-\varepsilon_i)\sum_{j=1}^{N} J_j F_{ji} \,. \tag{18}$$

Clearly the solution of the problem involves recurrence of radiosity at a generic surface J_i. Exact solution therefore invokes solving the geometric series associated with multiple (infinite) radiative reflections. Rewrite Eq. (18) as

$$M_i = J_i - (1-\varepsilon_i)\sum_{j=1}^{N} J_j F_{ji} = \sum_{j=1}^{N} J_j \Gamma_{ji} \,, \tag{19}$$

where $\Gamma_{ij} = \delta_{ij} - (1-\varepsilon_i) F_{ij}$. The matrix Γ_{ij} always has an inverse, which is denoted as $\left[\Psi_{ij}\right] = \left[\Gamma_{ij}\right]^{-1}$. Thus for each facet, we have

$$J_i = \sum_{j=1}^{N} M_j \Psi_{ji}, I_i = \frac{J_i - M_i}{1-\varepsilon_i}, \tag{20}$$

and

$$Q_i = \begin{cases} \sum_{j=1}^{N} F_{ji} M_j - M_i & \text{if } \varepsilon_i = 1 \\ \dfrac{\varepsilon_i \sum_{j=1}^{N} \Psi_{ji} M_j - M_i}{1-\varepsilon_i} & \text{if } \varepsilon_i \neq 1 \end{cases} . \tag{21}$$

For each facet, the material emissivity and temperature are known quantities. For diffusive thermal radiation, the emittance is diffuse and longwave in nature, and can thus be expressed using Boltzmann's law:

$$M_i = \varepsilon_i \sigma T_i^4 , \tag{22}$$

where σ = 5.67×10^{-8} W m^{-2} K^{-4} is the Stephen-Boltzmann constant. Note that Eqs. (20)-(21) represent the matrix solution of radiative heat exchange between canyon facets. When the view factor matrix F_{ij} is analytically determined, these solutions are hereafter referred

211 to as “exact” for they analytically resolves *infinite* number of reflections between canyon
212 surfaces through matrix inversion.
213

214 3. Model Validation

215 In this section, we first examine that if the radiative view factors predicted by Monte
216 Carlo algorithm agree with the analytical values for a bare street canyon absent of trees.
217 Next, the predicted view factors are used in the matrix method for prediction of net
218 radiation arising from canyon facets under thermal equilibrium. Lastly, the validated
219 Monte Carlo algorithm will be applied to estimate ground and wall temperatures in a real
220 street canyon during a night cooling episode.
221

222 3.1. Estimation of radiative view factors

223 The numerical algorithm for estimating view factors using Monte Carlo simulations
224 (MCS) is outlined in Eqs. (8)-(14). Using random samples, the accuracy of Monte Carlo
225 method, as expected, improves with the sample size. Taking the view factor between sky
226 and ground F_{SG} as example, Figure 3 shows the model accuracy as a function of number of
227 samples. With a sample size of 1,000, MCS is capable of predicting the view factor with
228 reasonable accuracy, as compared to the analytical formulation, while MCS with a sample
229 size of 10,000 yields results with negligible discrepancy. For subsequent simulations, we
230 will use the sample size of 10,000. Predictions of other street canyon view factors exhibit
231 similar trend with respect to sample size. The comparisons of all four view factors between
232 urban facets by Monte Carlo and analytical methods are shown in Figure 4. The

discrepancy between predictions by the two methods is nearly indiscernible, for canyon aspect ratio H/W ranging from 0.01 to 100. Also note that the most drastic change of all four view factors occur around $H/W \sim 1.0$, and covers the practical range of actual street canyon dimensions around 0.2 to 10. This observation highlights the importance of accurate prediction of radiative view factors for real street canyons.

3.2. Net radiation of canyon facets in thermal equilibrium

With the view factors being accurately estimated by the Monte Carlo method, we then apply the method to predict the net radiation from each urban facet under thermal equilibrium, in conjunction with the matrix method outlined in Section 2.2. Emissivity is set to be 1.0 for sky (canyon top) $\varepsilon_W = \varepsilon_G = 0.95$, where subscripts W and G denote properties of walls and the ground, respectively. The surfaces enclosing the street canyon (c.f. Figure 2) are set to be in constant temperatures as: sky T_a = 300 K, ground T_G = 290 K, east wall T_{W1} = 290 K, and west well T_{W2} = 295 K. Note that these values are chosen rather arbitrarily for demonstration purpose, and they do not affect the accuracy of the model predictions. The results of comparison between the Monte Carlo and the exact methods, as functions of the canyon aspect ratio, are shown in Figure 5: here the exact solution refers to the combination of analytical formulation of view factors in Eqs. (4)-(7) and the matrix method for net radiation with infinite reflections in Section 2.2. It is clear that the MCS predictions are in good agreement with the exact solution. As a function of canyon aspect ratio, the most significant variation happens again around $H/W \sim 1.0$, indicating the view factors are dominating the radiative energy distribution among different street canyon facets. It is also noteworthy that the model is capable of resolving differences in surface

temperatures of two opposite walls, given that their net radiation can be accurately determined.

3.3. Transient nocturnal cooling episode

Given that the proposed model is capable of predicting both view factor and net radiation with good accuracy as compared to the analytical method, here we further test the model for its capability of predicting surface temperatures, in conjunction with numerical procedures for heat conduction. In this study, we adopt a spatially-analytical scheme for solving heat conduction through solid ground and walls, based on the Green's function approach (Wang et al., 2011a). The temperature distribution for a finite wall with one-dimensional (1D) spatial domain $0 \le x \le d$ where d is the wall thickness, is given by a convolution integral equation as (Carslaw and Jaeger 1959; Cole et al., 2011):

$$T_W(x,t) = T_{i,W} + \int_0^t q_1(t-\tau)\,dG(x,\tau) - \int_0^t q_2(t-\tau)\,dG(d-x,\tau), \qquad (23)$$

where q_1 and q_2 are the heat fluxes at the two surfaces of the wall; and G is the Green's function (fundamental) solution of a homogeneous heat conduction problem. For a finite wall with thickness d, the Green's function solution is given by

$$G(x,t) = \frac{2\sqrt{(\alpha t/\pi)}}{k}\sum_{n=-\infty}^{\infty}\exp\left[-\frac{(x-2nd)^2}{4\alpha t}\right], \qquad -\frac{1}{k}\sum_{n=-\infty}^{\infty}|x-2nd|\,\mathrm{erfc}\left(\frac{|x-2nd|}{2\sqrt{\alpha t}}\right) \qquad (24)$$

where k and α are the thermal conductivity and diffusivity, respectively; and erfc(.) is the complimentary error function. Equations (23)-(24) can be readily evaluated using

numerical integration, given the knowledge of boundary conditions q_1 and q_2, and the initial condition T_i. A detailed solution procedure for Green's function approach can be found in Wang et al. (2011a).

Note that canyon ground, unlike walls bounded by two (building interior and exterior) boundaries, can be treated as a 1D semi-infinite solid domain, bounded only at the upper surface with an effective adiabatic (zero flux) condition at the lower boundary (in deep soil). Thus the solution of surface temperature of the ground can be approximated by a closed-form formula (Nunez et al., 1976; Wang et al., 2011a), as

$$T_{s,G}(t) = T_{i,G} + Q_G \frac{2\sqrt{\alpha_G t / \pi}}{k_G}, \tag{25}$$

where T_s is the surface temperature; and Q_G is the net radiation received at the ground surface, as predicted using matrix method with infinite reflections by Eq. (21).

The proposed method is tested for a nocturnal cooling event in the Grand-view district of Vancouver, measured by Nunez and Oke (1976) during September 9-11, 1973. The street canyon dimensions are d = 0.3 m, H = 7.31 m, and W = 7.54 m. Thermal properties of walls and the ground are: $(\rho c_p)_W = 2.09\times10^6$ J K^{-1} m^{-3}, k_W = 1.6 W m^{-1} K^{-1}, $(\rho c_p)_G = 1.88\times10^6$ J K^{-1} m^{-3}, k_G = 1.6 W m^{-1} K^{-1}, where ρ an c_p are the density and specific heat; and $\varepsilon_W = \varepsilon_G$ = 0.95. The nocturnal cooling episode was measured after sunset with calm winds, so the short wave radiation, sensible and latent heat fluxes are neglected in both the measurement and modelling. The initial longwave radiation is measured as 339 W m^{-2}. Surface temperatures of the canyon walls and ground predicted by the combined numerical framework (Monte Carlo simulation of view factors, matrix method for net radiation, and Green's function approach for heat conduction), are compared with field

297 measurements, as shown in Figure 6. The overall agreement between model predictions
298 and observations is reasonably good, with temperature discrepancy less than 1 ^{o}C in
299 general.
300

301 # 4. Model applications and discussion

302 With the proposed numerical framework validated against benchmark radiative
303 transfer problems and in-situ measurements, we proceed to apply the model to street
304 canyons with shade trees. We first test the effect of tree crown sizes on view factors
305 between canyon facets, followed by its implications to surface temperature evolution and
306 building energy consumption given diurnal atmospheric forcing. Some of the assumptions
307 made in the proposed methods and future model extensions are also discussed.
308

309 ## 4.1. Effect of tree sizes on view factors

310 For simplicity, we ignore the size of tree trunks due to its relative small dimension as
311 compared to tree crowns. Further, in this study, tree crowns assume circular cross-sectional
312 shapes, as shown in Figure 2, with a radius of R_t. As the vertical variability is not explicitly
313 resolved in the 2D urban canyon, and subsequently in the single layer UCM adopted in
314 WRF, we do not account complex tree geometries, e.g. roof top shading and probabilistic
315 distribution of tree heights in this paper, such as those developed in multi-layer UCMs by
316 Krayenhoff et al (2014). With presence of trees in the street canyon, radiative exchange
317 between canyon facets will be partially "blocked" by tree crowns. Thus, trees will
318 effectively shade canyon facets by intercepting radiative rays, with their actual shading

effect depending on the size of the tree crowns. Figure 7 demonstrates this shading effect as a function of canyon aspect ratio. Note that even with a very small tree crown size (R_t/W = 0.1), all radiative view factors are effectively reduced. As tree crown size increases, more radiation will be intercepted by trees and view factors further decrease. In addition, the shading effect is more significant for shallower canyons (with smaller H/W ratios). This is because for deep canyons, walls in the street canyon are already presented an important factor for shading, and the additional shading by trees are less prominent.

4.2. Canyon temperature and building energy consumption

Next, we apply the combined numerical framework to test the effect of tree sizes on diurnal evolution of canyon temperatures and building energy use. The model is driven by in-situ measurement of atmospheric and radiative forcings at Maryvale, Phoenix, Arizona on 04 June 2012 (clear day), measured by an eddy covariance flux tower. More details on the instrumentation and data quality control of the field measurement can be found in Chow et al. (2014). Relevant models parameters are given by measurement or previous model calibration as: d = 0.3 m, H = 15 m, W = 20 m, k_G = 1.6 W m^{-1} K^{-1}, k_W = 1.3 W m^{-1} K^{-1}, $(\rho c_p)_W = 1.26\times10^6$ J K^{-1} m^{-3}, $(\rho c_p)_G = 2.00\times10^6$ J K^{-1} m^{-3}, and ε_W = ε_G = 0.95. Diurnal variation of the atmospheric temperature and net (shortwave + longwave) downwelling radiation at the canyon top is plotted in Figure 8(a).

Note that this paper is focused on the radiative exchange in a street canyon, so turbulent (sensible and latent) heat fluxes are not accounted in energy transport. For an arid city like Phoenix, latent heat during a clear day is usually very small (<10% of the

341 irradiance), while the sensible heat flux can be significant (maximum daily sensible heat is
342 300 W m^{-2} on June 04, 2012 in Phoenix). So the negligence of turbulent heat is a crude
343 assumption. To include sensible and latent heat in surface energy balance, it requires
344 sophisticated physical parameterization schemes involving wind velocity, surface
345 roughness, atmospheric stability, humidity, soil moisture, and complex hydrological
346 processes (precipitation, infiltration, and surface runoff) (see Wang et al., 2013). It remains
347 a challenging task to build a complete land surface model based on stochastic simulations
348 including all physical processes. Furthermore, the Monte Carlo algorithm assumes
349 completely random emission angles of a ray (see Eqs. (8)-(9)), i.e. canyon facets are
350 Lambertian and opaque, and radiative rays are diffusive. This is not the case when direct
351 solar radiation is first impinged on a canyon facet. A sun-lit wall when receiving
352 directional solar radiation, for example, is certainly at higher temperature than a shaded
353 wall. One way to include that effect is to estimate a "shadow length" in a street canyon as a
354 function of city location, canyon orientation, and time of the day (Kusaka et al., 2001).
355 Nevertheless, the assumption of diffusive radiation is valid for subsequent reflections using
356 the matrix method.

357 A comparison of model estimate of ground surface temperature and field
358 measurements is shown in Figure 8(b), with no tree shading in the model. Despite the
359 above-mentioned limitation of the model, its prediction is comparable with the
360 measurement (with a $R^2 = 0.945$). Next, we include shade trees in the canyon with different
361 crown sizes. The result of model predictions for diurnal evolution of canyon surface
362 temperatures is shown in Figure 9(a). The shading effect is clearly demonstrated in that
363 when the tree crown size increases, surface temperatures of wall and ground decrease. A

increase of crown size from 0.5 m to 1.0 m leads to the reduction of surface temperatures up to 6-7 ^{o}C around noon.

Given the temperature profile through the wall is calculated using the Green's function approach in Eq. (23), the conductive heat flux entering the building can be computed using Fourier's law,

$$q_W(x,t) = -k\frac{dT_W}{dx} = -k\left[\int_0^t q_1(t-\tau)\,dG'(x,\tau) - \int_0^t q_2(t-\tau)\,dG'(d-x,\tau)\right], \quad (26)$$

at $x = d$. This flux is a good indicator for energy consumption inside the building to offset the heat inflow/outflow through building envelop and to maintain the interior thermal comfort through operation of heating, ventilation, and air-conditioning systems. The model predicted heat flux entering the building through wall is presented in Figure 9(b), for various tree sizes. Again, it is clear that in the absence of trees, building interiors receives large heat inflow (positive) through the wall in a clear summer day (June 04). When trees are presented, the magnitude of heat inflow decreases significantly with the tree size, indicating the potential of shade trees for building energy saving.

5. Concluding remarks

A new numerical framework is developed for radiative heat exchange in street canyons with shade trees, by combining the Monte Carlo simulation of view factors and matrix method for infinite reflections. The model is validated against analytical solutions of benchmark radiative transfer problems as well as field measurements in real street canyons. Results of comparison show that the model is of capable of predicting radiative view

385 factors, surface temperatures, and net radiation of canyon facets with good accuracy, in
386 both steady state and transient cases. We then apply the model to study the effect of shade
387 trees and their sizes on the diurnal evolution of canyon surface temperatures in conjunction
388 with a Green's function approach for heat conduction. It is manifested that shade trees are
389 effective in reducing canyon surface temperatures, with the shading effect enhanced by
390 increasing tree sizes. The presence of trees in a street canyon demonstrates good potential
391 in reducing cooling energy consumption as it mitigates the heat inflow into the building
392 through walls.

393 In addition, Monte Carlo method is also a powerful tool in computing absorption and
394 scattering of radiation if complex participating media (e.g. dust, soot, pollen, etc.) are
395 presented in street canyons. By randomizing radiation using energy bundles, scattering
396 deflects a ray's direction, and absorption causes a ray to be intercepted. The frequency,
397 direction, and fraction of attenuation due to either scattering or absorption can be simulated
398 by random numbers and as functions of scattering or absorption coefficients. This
399 treatment is particularly useful for cities with heavy atmospheric pollution, either caused
400 by natural sources with seasonal occurrence or by constant industrial sources. By inclusion
401 of participating media, numerical models will improve accuracy in simulating radiative
402 exchange and thermal field in an urban canopy layer, which will subsequently enhance
403 numerical capacity in, e.g. building energy model or land-atmosphere interactions.

Acknowledgements

This work is supported by the National Science Foundation (NSF) under grant number CBET-1435881. Partial financial support by the Central Arizona-Phoenix Long-Term Ecological Research (CAP LTER) project under NSF grant CAP3: BCS-1026865 is gratefully acknowledged.

References:

Akbari, H., Pomerantz, M., Taha, H., 2001. Cool surfaces and shade trees to reduce energy use and improve air quality in urban areas. Sol. Energy 70, 295-310.

Aoyagi, T., Takahashi, S., 2012. Development of an urban multilayer radiation scheme and its application to the urban surface warming potential. Boundary-Layer Meteorol. 142, 305-328.

Arnfield, A.J., 2003. Two decades of urban climate research: A review of turbulence, exchanges of energy and water, and the urban heat island. Int. J. Climatol. 23, 1-26.

Carslaw, H.S., Jaeger, J.C., 1959. Conduction of Heat in Solids. Oxford University Press Oxford, 510pp.

Chen, F., Kusaka, H., Bornstein, R., Ching, J., Grimmond, C.S.B., Grossman-Clarke, S., Loridan, T., Manning, K.W., Martilli, A., Miao, S.G., Sailor, D., Salamanca, F.P., Taha, H., Tewari, M., Wang, X.M., Wyszogrodzki, A.A., Zhang, C.L., 2011. The integrated WRF/urban modelling system: development, evaluation, and applications to urban environmental problems. Int. J. Climatol. 31, 273-288.

Chow, W.T., Volo, T.J., Vivoni, E.R., Jenerette, G.D., Ruddell, B.L., 2014. Seasonal dynamics of a suburban energy balance in Phoenix, Arizona. Int. J. Climatol. Published online, DOI:10.1002/joc.3947.

Cole, K.D., Haji-Sheikh, A., Beck, J.V., Litkouhi, B., 2011. Heat Conduction using Green's Functions. Taylor & Francis Boca Raton, 653pp.

Grimmond, C.S.B., Blackett, M., Best, M.J., Baik, J.J., Belcher, S.E., Beringer, J., Bohnenstengel, S.I., Calmet, I., Chen, F., Coutts, A., Dandou, A., Fortuniak, K., Gouvea, M.L., Hamdi, R., Hendry, M., Kanda, M., Kawai, T., Kawamoto, Y., Kondo,

H., Krayenhoff, E.S., Lee, S.H., Loridan, T., Martilli, A., Masson, V., Miao, S., Oleson, K., Ooka, R., Pigeon, G., Porson, A., Ryu, Y.H., Salamanca, F., Steeneveld, G.J., Tombrou, M., Voogt, J.A., Young, D.T., Zhang, N., 2011. Initial results from Phase 2 of the international urban energy balance model comparison. Int. J. Climatol. 31, 244-272.

Grimmond, C.S.B., Blackett, M., Best, M.J., Barlow, J., Baik, J.J., Belcher, S.E., Bohnenstengel, S.I., Calmet, I., Chen, F., Dandou, A., Fortuniak, K., Gouvea, M.L., Hamdi, R., Hendry, M., Kawai, T., Kawamoto, Y., Kondo, H., Krayenhoff, E.S., Lee, S.H., Loridan, T., Martilli, A., Masson, V., Miao, S., Oleson, K., Pigeon, G., Porson, A., Ryu, Y.H., Salamanca, F., Shashua-Bar, L., Steeneveld, G.J., Tombrou, M., Voogt, J., Young, D., Zhang, N., 2010. The international urban energy balance models comparison project: First results from Phase 1. J. Appl. Meteorol. Climatol. 49, 1268-1292.

Grimmond, C.S.B., Oke, T.R., 1999. Aerodynamic properties of urban areas derived from analysis of surface form. J. Appl. Meteorol. 38, 1262-1292.

Harman, I.N., Best, M.J., Belcher, S.E., 2004. Radiative exchange in an urban street canyon. Boundary-Layer Meteorol. 110, 301-316.

Howell, J.R., 1968. Application of Monte Carlo to heat transfer problems, in: Irvine Jr., T.F., Hartnett, J.P. (Eds.) Advances in Heat Transfer, Vol 5, Academic Press, New York, pp. 54.

Howell, J.R., 1998. The Monte Carlo method in radiative heat transfer. J. Heat Transf. 120, 547-560.

Kikegawa, Y., Genchi, Y., Yoshikado, H., Kondo, H., 2003. Development of a numerical simulation system toward comprehensive assessments of urban warming countermeasures including their impacts upon the urban buildings' energy-demands. Appl. Energy 76, 449-466.

Krayenhoff, E.S., Christen, A., Martilli, A., Oke, T.R., 2014. A multi-layer radiation model for urban neighbourhoods with trees. Boundary-Layer Meteorol. 151, 139-178.

Kusaka, H., Kondo, H., Kikegawa, Y., Kimura, F., 2001. A simple single-layer urban canopy model for atmospheric models: Comparison with multi-layer and slab models. Boundary-Layer Meteorol. 101, 329-358.

Lemonsu, A., Masson, V., Shashua-Bar, L., Erell, E., Pearlmutter, D., 2012. Inclusion of vegetation in the Town Energy Balance model for modelling urban green areas. Geosci. Model Dev. 5, 1377-1393.

Li, Z.Q., Xia, X.G., Cribb, M., Mi, W., Holben, B., Wang, P.C., Chen, H.B., Tsay, S.C., Eck, T.F., Zhao, F.S., Dutton, E.G., Dickerson, R.R., 2007. Aerosol optical properties and their radiative effects in northern China. J. Geophys. Res.-Atmos. 112, D22S01.

Nunez, M., Oke, T.R., 1976. Long-wave radiative flux divergence and nocturnal cooling of the urban atmosphere. Boundary-Layer Meteorol. 10, 121-135.

Ouldboukhitine, S.E., Belarbi, R., Sailor, D.J., 2014. Experimental and numerical investigation of urban street canyons to evaluate the impact of green roof inside and outside buildings. Appl. Energy 114, 273-282.

Prabhakar, G., Betterton, E.A., Conant, W., Herman, B.M., 2014. Effect of urban growth on aerosol optical depth - Tucson, Arizona, 35 years later. J. Appl. Meteorol. Climatol. 53, 1876-1885.

478 Robinson, D., Stone, A., 2004. Solar radiation modelling in the urban context. Sol. Energy
479 77, 295-309.
480 Robinson, D., Stone, A., 2005. A simplified radiosity algorithm for general urban radiation
481 exchange. Building Serv. Eng. Res. Technol. 26, 271-284.
482 Robinson, D., Stone, A., 2006. Internal illumination prediction based on a simplified
483 radiosity algorithm. Sol. Energy 80, 260-267.
484 Sailor, D.J., Resh, K., Segura, D., 2006. Field measurement of albedo for limited extent
485 test surfaces. Sol. Energy 80, 589-599.
486 Santamouris, M., 2014. Cooling the cities - A review of reflective and green roof
487 mitigation technologies to fight heat island and improve comfort in urban
488 environments. Sol. Energy 103, 682-703.
489 Santamouris, M., Papanikolaou, N., Livada, I., Koronakis, I., Georgakis, C., Argiriou, A.,
490 Assimakopoulos, D.N., 2001. On the impact of urban climate on the energy
491 consumption of buildings. Sol. Energy 70, 201-216.
492 Sparrow, E.M., Cess, R.D., 1978. Radiation Heat Transfer, Augmented Ed., HarperCollins,
493 London, UK.
494 Sun, Y.L., Zhuang, G.S., Tang, A.H., Wang, Y., An, Z.S., 2006. Chemical characteristics
495 of PM2.5 and PM10 in haze-fog episodes in Beijing. Environ. Sci. Technol. 40, 3148-
496 3155.
497 Synnefa, A., Santamouris, M., Apostolakis, K., 2007. On the development, optical
498 properties and thermal performance of cool colored coatings for the urban
499 environment. Sol. Energy 81, 488-497.

Taha, H., 1997. Urban climates and heat islands: Albedo, evapotranspiration, and anthropogenic heat. Energy Build. 25, 99-103.

United Nations, 2012. World urbanization prospects: The 2011 revision, The United Nations' Department of Economic and Social Affairs - Population Division, New York, pp. 33.

Wang, Z.H., 2010. Geometric effect of radiative heat exchange in concave structure with application to heating of steel I-sections in fire. Int. J. Heat Mass Transf. 53, 997-1003.

Wang, Z.H., Bou-Zeid, E., Smith, J.A., 2011a. A spatially-analytical scheme for surface temperatures and conductive heat fluxes in urban canopy models. Boundary-Layer Meteorol. 138, 171-193.

Wang, Z.H., Bou-Zeid, E., Au, S.K., Smith, J.A., 2011b. Analyzing the sensitivity of WRF's single-layer urban canopy model to parameter uncertainty using advanced Monte Carlo simulation. J. Appl. Meteorol. Climatol. 50, 1795-1814.

Wang, Z.H., Bou-Zeid, E., Smith, J.A., 2013. A coupled energy transport and hydrological model for urban canopies evaluated using a wireless sensor network. Q. J. R. Meteorol. Soc. 139, 1643-1657.

Wong, N.H., Jusuf, S.K., Syafii, N.I., Chen, Y.X., Hajadi, N., Sathyanarayanan, H., Manickavasagam, Y.V., 2011. Evaluation of the impact of the surrounding urban morphology on building energy consumption. Sol. Energy 85, 57-71.

Yang, W.-J., Taniguchi, H., Kudo, K., 1995. Radiative heat transfer by the Monte Carlo method, in: Hartnett, J.P., Irvine, T.F. (Eds.) Advances in Heat Transfer, Vol 27, Academic Press, San Diego, pp. 1-215.

Caption of Figures:

Figure 1. Schematic of radiative transfer between two generic surfaces

Figure 2. Cross sectional view of 2D street canyon with trees. The cross section of tree crowns is simplified as circles with radius R_t.

Figure 3. Effect of sample size on Monte Carlo prediction of view factor F_{SG}: (a) as a function of canyon aspect ratio, and (b) as a function of sample sizes at $H/W = 1.0$.

Figure 4. View factors of radiative heat exchange between canyon facets as functions of the canyon aspect ratio H/W; subscripts S, G, and W denote sky, ground, and wall, respectively. The sample size is 10,000 for the Monte Carlo simulations.

Figure 5. Comparison of net radiation of different canyon facets at thermal equilibrium, as predicted by the exact and the proposed hybrid methods. Surface of the four enclosing surfaces are set as $T_a = 300$ K, $T_G = 290$ K, $T_{W1} = 290$ K and $T_{W2} = 295$ K.

Figure 6. Comparison of averaged wall and ground temperatures predicted by the model and field measurements in the canyon during the night cooling episode.

Figure 7. Monte Carlo simulation of view factors of radiative heat exchange between canyon facets with trees, as functions of the canyon aspect ratio H/W. In this case, the canyon width W is fixed as 20 m, and the centre of tree crown height is located at $H/2$.

Figure 8. Model application with (a) radiative forcing measured on 04 June 2012, Phoenix, AZ, and (b) comparison between model prediction and measurement of ground surface temperature.

Figure 9. Model prediction of diurnal variation of (a) surface temperatures, and (b) heat conducted into building through walls. Diurnal radiative forcing is the same as in Figure 8.

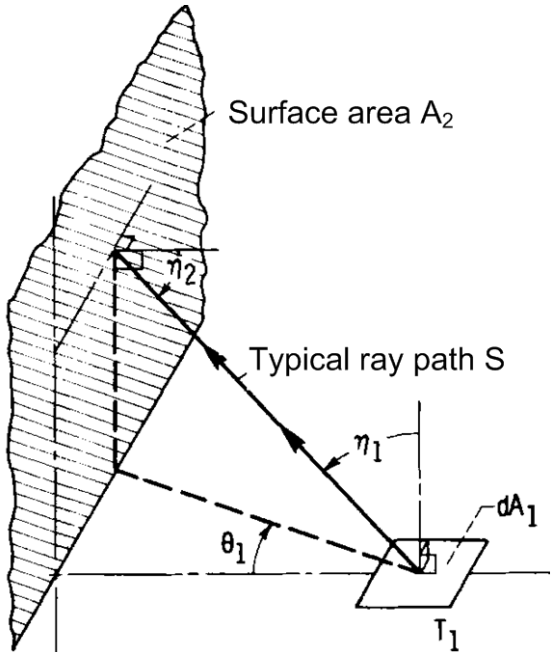

Figure 1. Schematic of radiative transfer between two generic surfaces

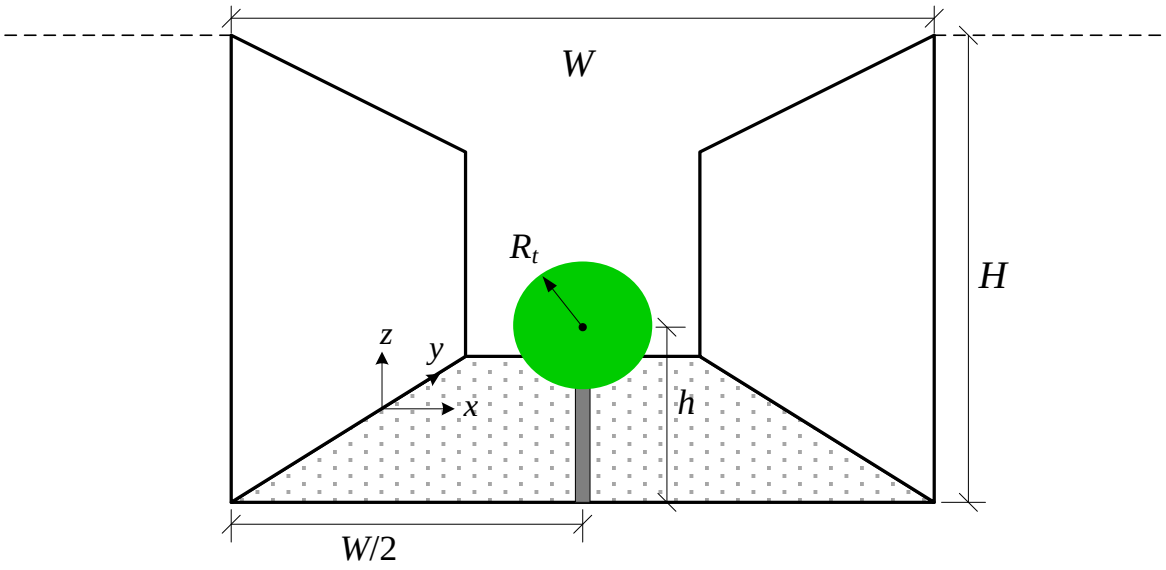

551

552 **Figure 2**. Cross sectional view of 2D street canyon with trees. The cross section of tree

553 crowns is simplified as circles with radius R_t.

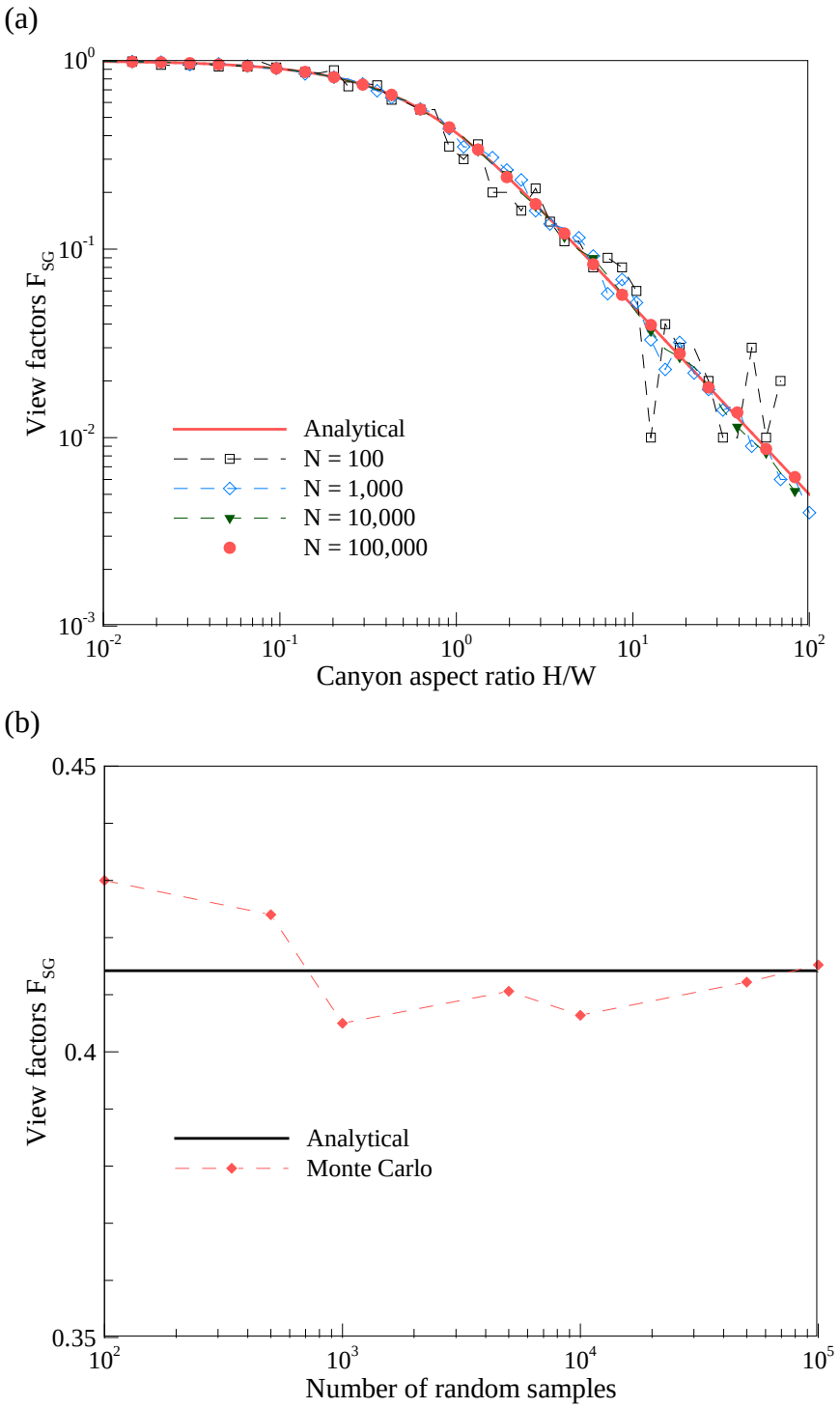

554

555 **Figure 3**. Effect of sample size on Monte Carlo prediction of view factor F_{SG}: (a) as a

556 function of canyon aspect ratio, and (b) as a function of sample sizes at $H/W = 1.0$.

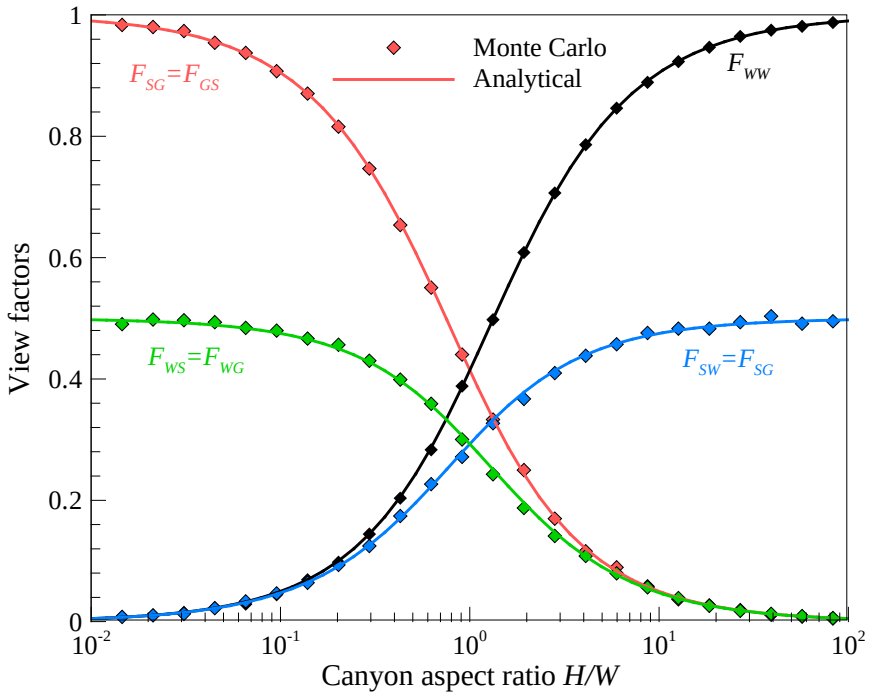

557

558 **Figure 4**. View factors of radiative heat exchange between canyon facets as functions of

559 the canyon aspect ratio H/W; subscripts S, G, and W denote sky, ground, and wall,

560 respectively. The sample size is 10,000 for the Monte Carlo simulations.

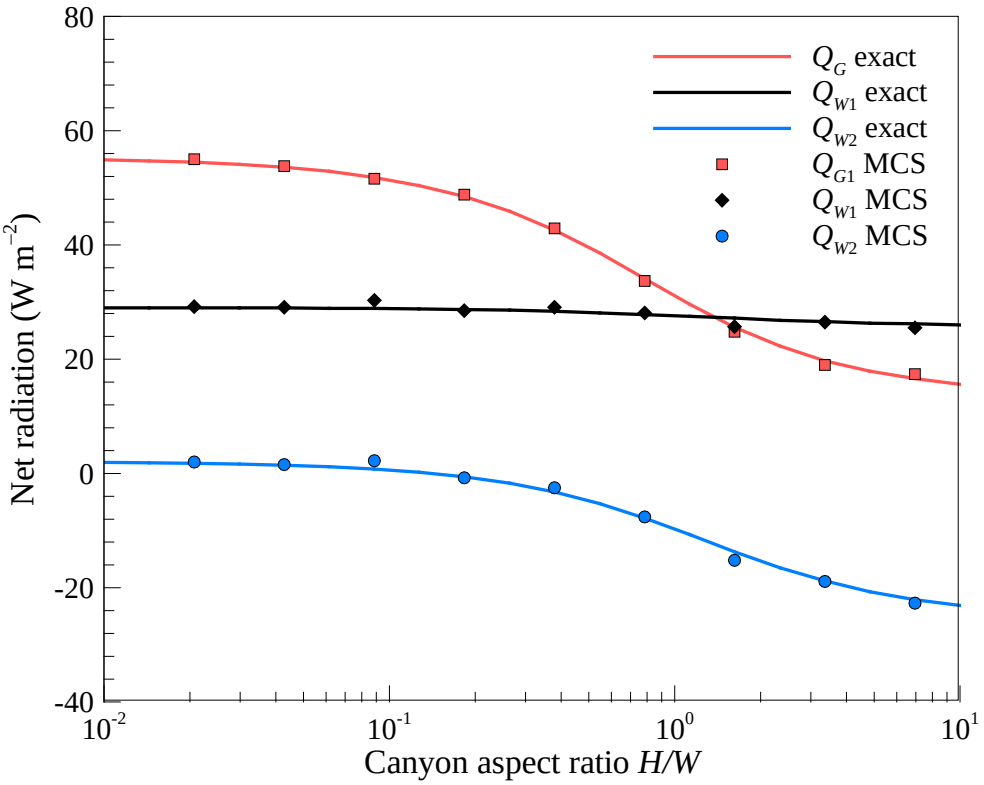

561

562 **Figure 5**. Comparison of net radiation of different canyon facets at thermal equilibrium, as

563 predicted by the exact and the proposed hybrid methods. Surface of the four enclosing

564 surfaces are set as T_a = 300 K, T_G = 290 K, T_{W1} = 290 K and T_{W2} = 295 K.

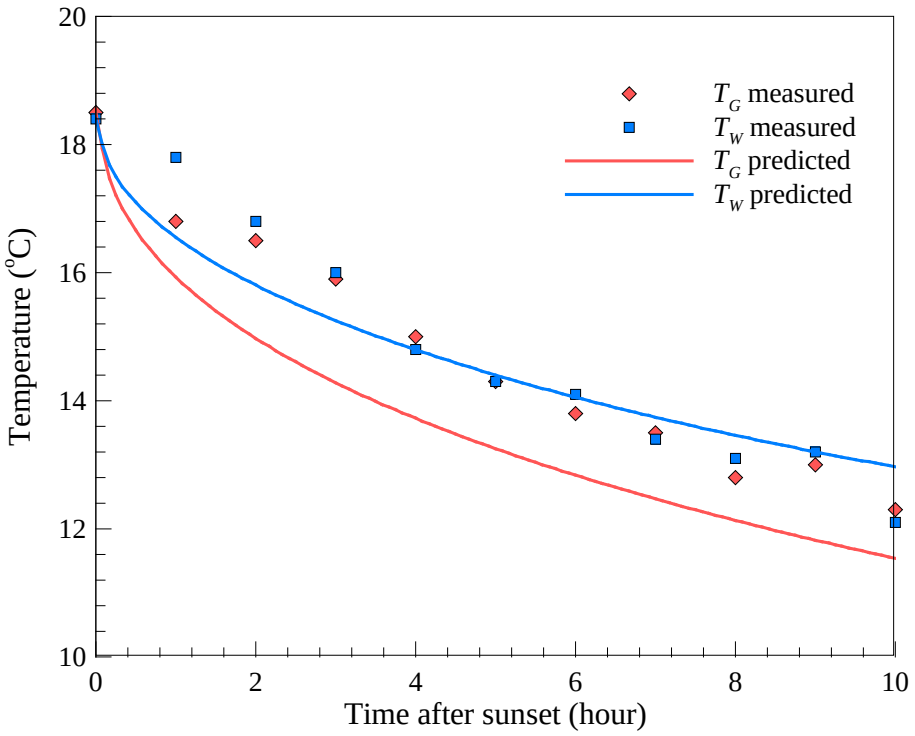

565

566 **Figure 6**. Comparison of averaged wall and ground temperatures predicted by the model

567 and field measurements in the canyon during the night cooling episode.

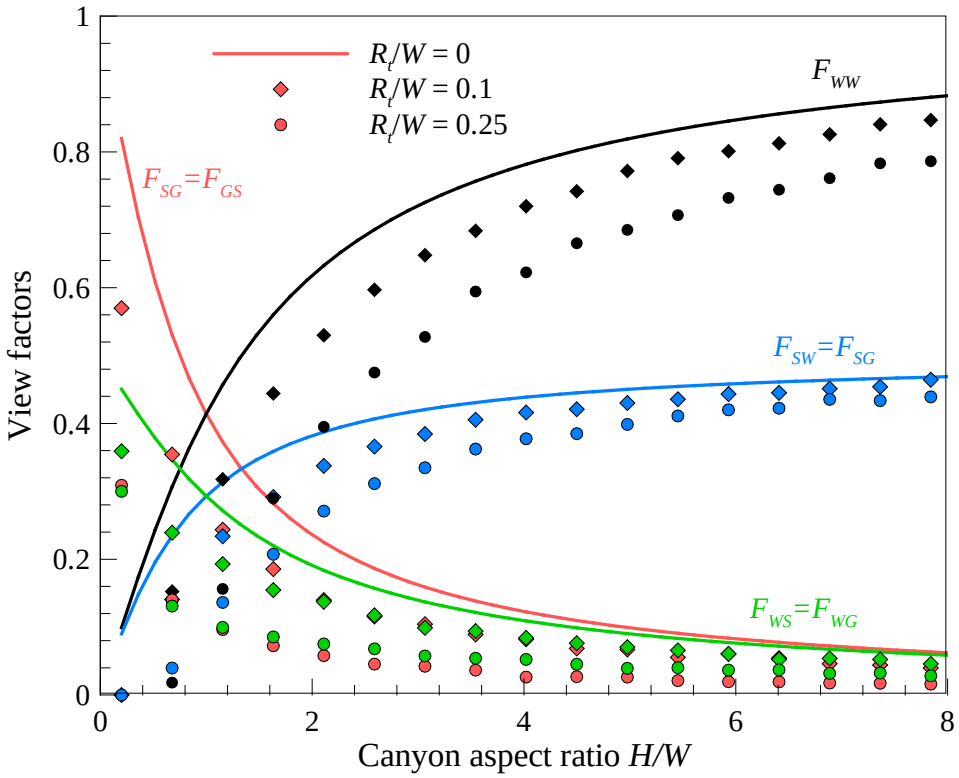

568

569 **Figure 7**. Monte Carlo simulation of view factors of radiative heat exchange between

570 canyon facets with trees, as functions of the canyon aspect ratio H/W. In this case, the

571 canyon width W is fixed as 20 m, and the centre of tree crown height is located at $H/2$.

(a)

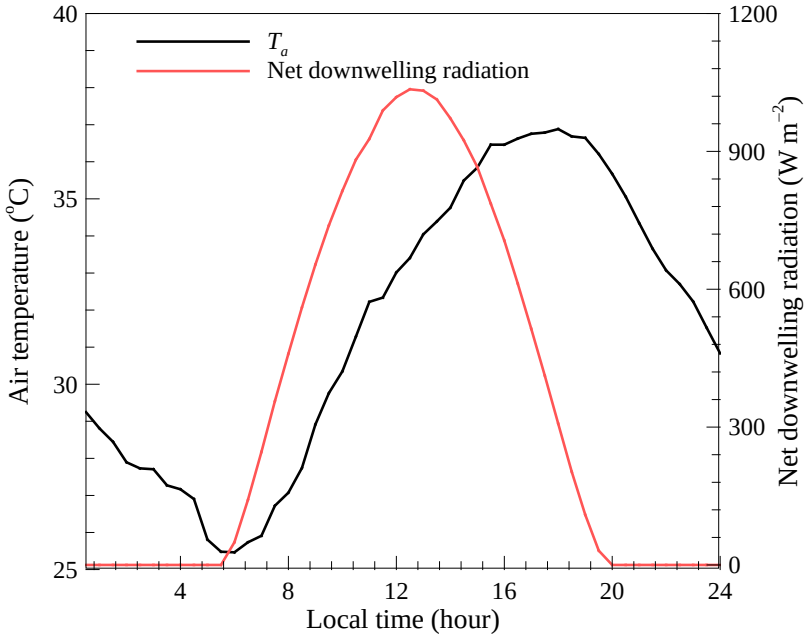

(b)

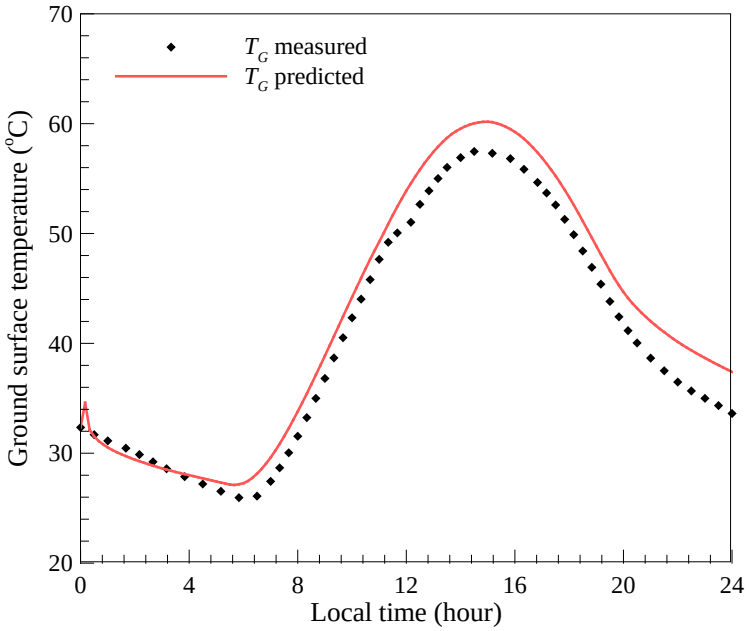

572

573 **Figure 8**. Model application with (a) radiative forcing measured on 04 June 2012, Phoenix,

574 AZ, and (b) comparison between model prediction and measurement of ground surface

575 temperature.

(a)

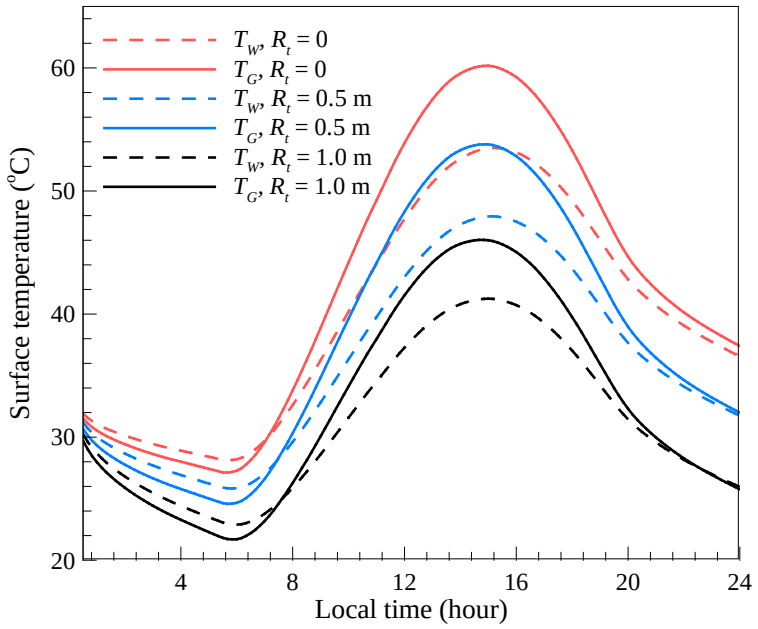

(b)

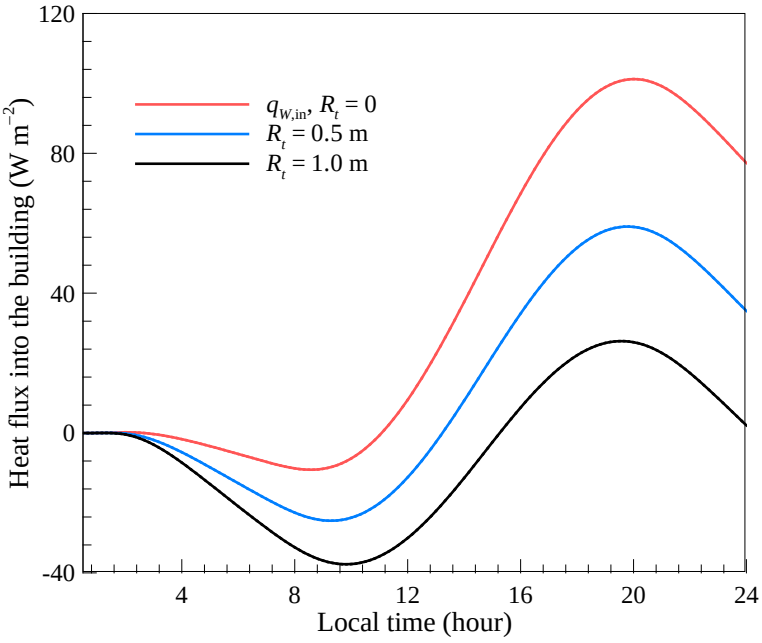

576

577 **Figure 9**. Model prediction of diurnal variation of (a) surface temperatures, and (b) heat

578 conducted into building through walls. Diurnal radiative forcing is the same as in Figure 8.